HiSST: 2nd International Conference on
High-Speed Vehicle Science Technology
11–15 September 2022, Bruges, Belgium

High-Speed system modelling, simulating and in-flight test

L. Galembeck [1], J.B.M. Cavalcanti[1], B.O. Silva[1], A. Passaro[1], A.C. Fraile Jr. [1], M.Z.J. Ferreira[1], C.H.M. Souza[2], D.J.F.V. Boas[2], C.B. Mendonça[2], J. Steelant[3]

Abstract

This paper presents a system identification chain of a hypersonic glide vehicle in low Mach numbers (below Mach 2). The system was modelled and simulated using Computational Fluid Dynamics (CFD) using Fluent® as software, with density and pressure-based solvers to obtain its aerodynamic coefficients for simulation and control purposes. A 1st and 2nd order spatial discretization was made to generate the meshes with around 7.5 million elements and a Spalart-Allmaras turbulence method was used. The complete Aerodynamic database will be obtained after computing the stability derivatives using the Vortex Lattice Method (VLM). With the aerodynamic coefficients it's possible to load the glider model in a simulation environment, developed in Matlab Simulink, and check the behaviour of the aircraft in flight. Using the simulation environment and control system techniques it is possible to develop a control system able to manage the vehicle in different conditions below Mach 2 until splash-down. An external layer is then added to the control algorithm in order to perform a parameter identification in-flight experiment when the correct conditions are obtained. The experiment is planned to perform a series of doublet manoeuvres at Mach 2 and Mach 1.35. After the flight the embedded sensors data will be analysed and compared to the numerical model in Simulink aiming to improve the model within the limits of the experiment.

Keywords: *Aerodynamics, glider, In-flight test, system identification, GNC*

Nomenclature

A	Axial force
AEDB	Aerodynamical Database
AoA	Angle of attack
b	Wing span
CFD	Computational Fluid Dynamics
C_D	Drag force coefficient
C_L	Lift force coefficient
C_l	Rolling moment coefficient
C_m	Pitching moment coefficient
C_n	Yawing moment coefficient
c_p	Specific heat at constant pressure
D	Drag force
EFTV	Experimental Flight Test Vehicle
ESM	Experimental Service Module
FCC	Flight Control Computer
GNC	Guidance Navigation Control
L	Lift force
L_{ref}	Reference length
LQI	Linear Quadratic Integral
LQR	Linear Quadratic Regulator
LRF	Layout reference frame
MRC	Moment reference center
M_l	Rolling moment
M_m	Pitching moment
M_n	Yawing moment
N	Normal force
S	Surface area
T	Temperature
V	Velocity
α	Angle of attack
β	Angle of sideslip
δ	Elevon deflection

Subscripts

∞	freestream conditions

[1] *IEAV, Aerothermodynamics and Hypersonic Division, Trevo José Alberto Albano do Amarante, n° 1 12.228-001, São José dos Campos, Brazil, galembecklg@fab.mil.br, cavalcantijbmc@fab.mil.br, brenobos@fab.mil.br, angelopassaro@fab.mil.br, fraileacfj@fab.mil.br, marcoszottimzjf@fab.mil.br*

[2] *IAE, Institute of Aeronautics and Space, Pç Mal. Eduardo Gomes 50, São José dos Campos, SP, 12228-904, Brazil, souzachms@fab.mil.br, dantondjfvb@fab.mil.br, celsobdm@gmail.com*

[3] *ESA-ESTEC, Aerothermodynamics and Propulsion Analysis Section TEC-MPA, P.O. Box 299, Noordwijk, Netherlands, Johan.Steelant@esa.int*

1. Introduction

The HEXAFLY-INT (High-Speed Experimental Fly Vehicles - INTernational) Project is an international consortium with partners from the European Union, Brazil and Australia aiming to develop and increase TRL level for key technologies to High-Speed transportation. Hypersonic speeds could make a regular flight from Brussels to Sydney being reduced to only 2h47m. Several challenges need to be faced when developing high-speed vehicles. Hence the vehicle design, manufacturing, assembly and verification are carefully studied allowing the hypersonic glider to demonstrate a high aerodynamic efficiency in combination with high internal volume; a gliding flight capability at a cruise Mach number of 7 to 8 in a controlled way; optimal use of advanced high-temperature materials and/or structures; and an evaluation of the sonic boom [1,3].

The Hypersonic glider will be launched from CLA (Alcantara Launch Center) in Brazil, by the 13-ton solid Brazilian sounding rocket, the VBS-50. The suborbital flight profile will reach an apogee around 100km where the payload will be released. The Experimental Flight Test Vehicle (glider) will be assisted by an Experimental Support Module (ESM) containing a Cold Gas System able to control the train (glider+ESM) attitude until the dynamic pressure is high enough to allow the aerodynamic surfaces to manoeuvre the glider. At this point (around 50km of altitude), the ESM will be ejected, and the glider will perform a pull-up manoeuvre to reach the experimental window at 30km at a Mach between 7 and 8. Fig 1 shows the 4m long with 1.2m wingspan train (left), glider associated with the ESM module, and the flight profile (right). After the pull up, the EFTV glider will execute banking manoeuvres to keep a safe distance from the Brazilian shore but, at the same, keeping the vehicle inside the telemetry stations range [2]. When the vehicle reaches Mach 2 at around 20km of altitude, a Brazilian-developed control algorithm will be switched on in order to perform a series of system identification in-flight experiments until the splash down in the ocean.

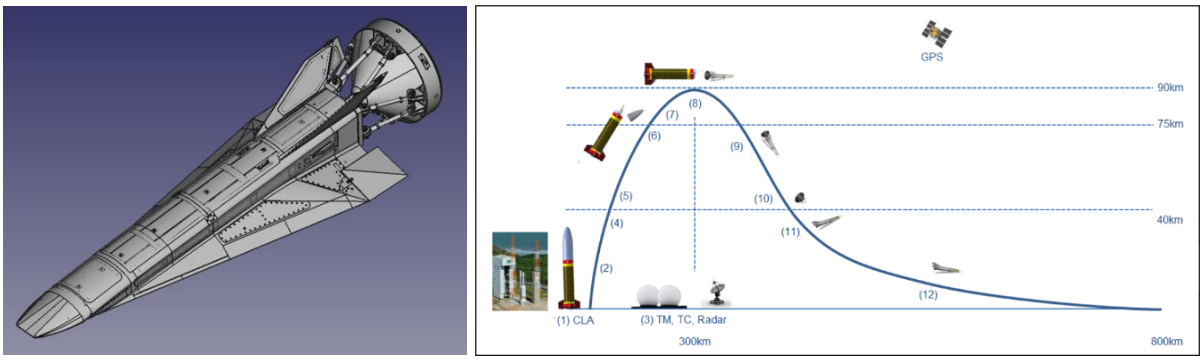

Fig 1 – Hexafly-Int EFTV+ESM (left) and mission profile (right).

Above Mach 2, coefficients were obtained through a combination of CFD simulations made by CIRA, ESA, DLR and experimental (wind tunnel) data provided by TsAGI [4, 5]. This dataset was cross-checked and compiled in a database called AEDB, which held data from Mach 2 to 9, comprising different values of AoA, AoS, and positions of elevons. Fig. 1 shows the flight profile intended for the flight test. Unfortunately, there was a lack of data for the flight below Mach number 2.

A new set of CFD computations has been carried out to evaluate the extension of the in-flight test below Mach 2 until the splashdown. These computations allow the determination of the aerodynamic forces and moments actuating during the vehicle's flight, which can be modelled through aerodynamic coefficients. These coefficients are related by dimensionless factors.

Fig. 2, adapted from reference [4], shows the layout reference frame (LRF) used in the computations in addition to the moment reference centre (MRC), whose coordinates are (xLRF, yLRF, zLRF) = (1.455, 0, 0.12) (m).

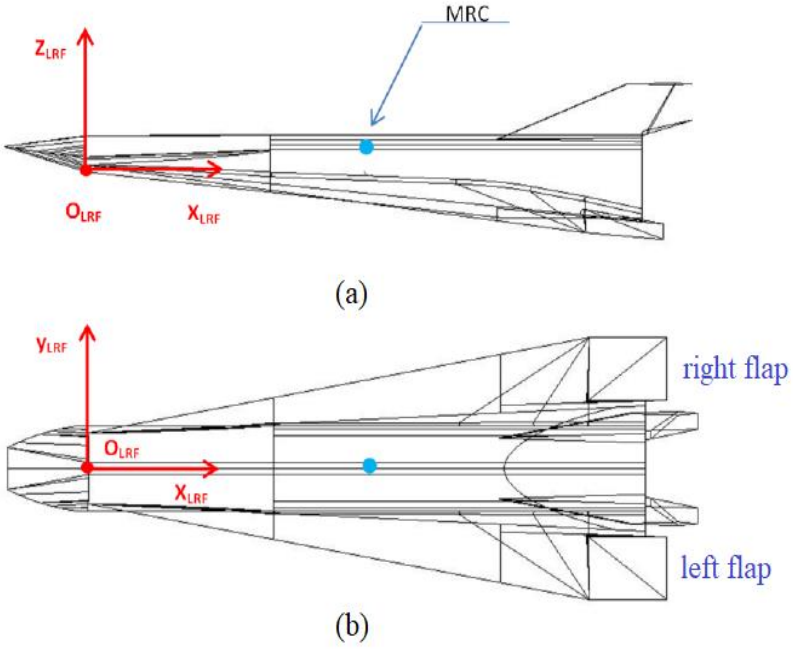

Fig 2 – Layout reference frame (LRF) used in our computational domain, in addition to the moment reference centre (MRC). Adapted from reference [4].

Aerodynamic forces are calculated along the LRF axes considering contributions from both pressure and viscous forces. Lift (L) and drag (D) forces are then obtained in the wind reference frame, and lift and drag coefficients can be calculated from the following expressions:

$$C_L = \frac{L}{0.5\rho_\infty V_\infty^2 S} \tag{1}$$

$$C_D = \frac{D}{0.5\rho_\infty V_\infty^2 S} \tag{2}$$

In equations (1) and (2), ρ_∞ and V_∞ are the density and the velocity calculated at freestream conditions and S = 2.52 m^2 is the reference area.
Aerodynamic moment coefficients are calculated around the MRC with the equations:

$$C_l = \frac{M_l}{0.5\rho_\infty V_\infty^2 b S} \tag{3}$$

$$C_m = \frac{M_m}{0.5\rho_\infty V_\infty^2 L_{ref} S} \tag{4}$$

$$C_n = \frac{M_n}{0.5\rho_\infty V_\infty^2 b S} \tag{5}$$

In equations (3) to (5), M_l, M_m, and M_n are the rolling, pitching and yawing moments around the MRC, b = 1.24 m is the wing span and L_{ref} = 3.29 m is the reference length.

2. Methodology

The methodology for determining the aerodynamic coefficients comprises studies of mesh convergence and code-to-code validation. In the first part, meshes with different numbers of elements are used, and the resulting coefficients are compared. The regular mesh size that presents acceptable results is used

in subsequent simulations. Two CFD solvers (density and pressure based), existing in Ansys Fluent® software package, are also evaluated.

The next step encompasses a code-to-code validation. Results of some cases already solved by the European consortium are compared with the ones obtained in this study, with different meshes. The two solvers (pressure and density based) are compared. In both cases, 2nd order spatial discretisation and the Spalart-Allmaras turbulence method are used. This step allows the choice of the adequate solver for the third step, balancing the simulation results quality and the computer processing time.

After that, several cases with the flow conditions of Mach number 1.35 and 15,884 m of altitude, various deflections of the control surfaces, angles of attack, and sideslip were simulated and the aerodynamic coefficients were obtained, resulting in 117 simulation cases.

The aerodynamic coefficients for these new conditions were not included in the available aerodynamic database (AEDB) [5]. The same models used to build the available AEDB were employed in this work, so air is considered a thermally perfect gas with specific heat at constant pressure depending on temperature, while the density is calculated using the ideal gas law [4, 5]. Pressure and temperature are approximately 10543 Pa and 216.65 K, respectively [6]. ANSYS Fluent® coupled pressure -based solver with second-order discretisation was used for this set of simulations. Laminar and turbulent viscosity are respectively calculated by Sutherland's law and the Spalart-Allmaras model [7]. All EFTV walls are considered adiabatic surfaces.

For symmetric configurations, such as when both left and right elevons have the same deflection or when the angle of sideslip (β) is zero, a computational domain containing a half body is assumed. On the other hand, for asymmetric elevon deflections or cases with $\beta \neq 0$, the entire body is included in the computational domain. Unstructured grids were used in all calculations. The exact number of cells for each grid depends on the elevon deflection and the domain type (half or full body). Grids with half body have approximately 7.6×10^6 cells, while those with the full body have 15×10^6 cells.

Simulations were performed for values of angle of attack (α) of -10, -5, 0, 5, and 10 deg. The sideslip angle is kept at 0, 2, or 4 deg. In all calculations, a combination of elevon deflections from -15 to 5 deg is considered.

The aerodynamic database (AEDB) will be later completed after the computation of the stability derivatives using the Vortex Lattice Method (VLM). The obtained aerodynamic coefficients dataset is going to be used in the flight dynamics and control simulations.

A 6-DoF simulator was developed in Matlab Simulink® for a WGS-84 rotating frame, with the environmental inputs as the gravity and atmospheric model, being established according to [8] and NRLMSISE-00 based models. The state variables used were the position, euler angles, rates of roll, pitch and yaw, and angular velocities. Stability derivatives will be obtained with a simplified geometry simulated with a VLM code.

The next phase comprises the development of a latero-directional and longitudinal flight controller using linear control techniques. The flight simulator and the complete AEDB (below Mach 2) will be used to develop a controller able to guide the aircraft under different flight conditions having Fig. 3 as an example of a possible implementation where the matrices A, B, C and D represent a state-space model. K and Ki are the gains obtained from the Riccati equation.

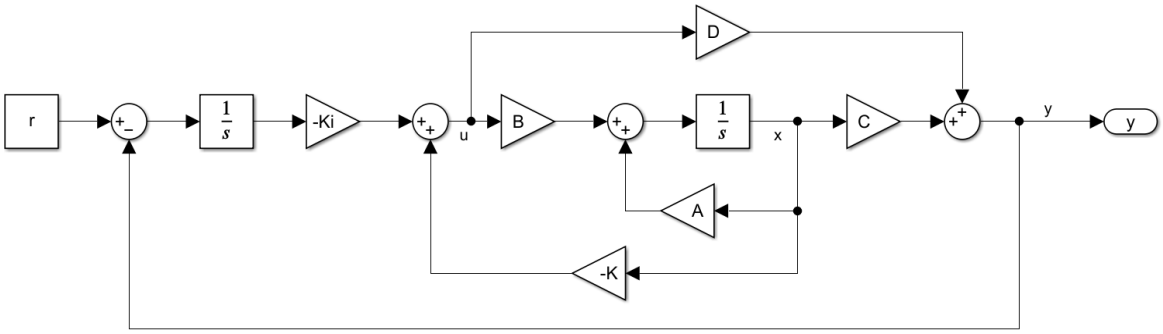

Fig 3 – LQI controller

Finally, an extra software layer will be loaded in the Flight Control Computer in order to command the Parameter IDentification (PID) experiment in the fight when the right conditions are obtained. Fig 4 shows an example of the excitation architecture.

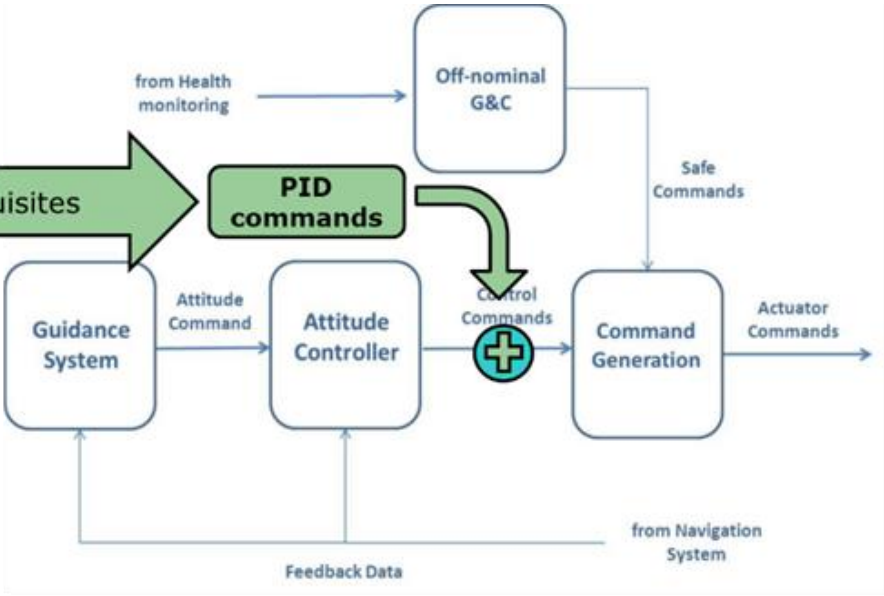

Fig 4 – Parameter Identification excitation illustrative architecture.

The PID commands will be based on a multistep input strategy able to excite longitudinal and lateral-directional modes. The pressure field around the aircraft surface varies according to a few parameters which dictate aircraft behaviour, and that is characterised in terms of aerodynamic stability and control derivatives. Aircraft geometry, angle of attack, angle of sideslip, Mach number and dynamic pressure are some factors that affect flight stability.

In high-speed vehicles flight evaluation, the Mach number variation is also a factor of concern. That happens because it strongly affects not only stability and control derivatives, but also vehicle stability, as an outcome of Mach dependencies. An additional challenge in parameter identification for high-speed flight is the rapid variations of flight conditions, leading to a short window to excite and collect data from a manoeuvre in a highly nonlinear behaviour condition.

The aircraft parameter estimation is formulated as a parametric modelling problem. The glider is modelled by a set of dynamic equations containing unknown parameters. To determine the unknown parameters the aircraft is excited by a suitable input and the actual aircraft response (output) is measured. The unknown parameters of the model are inferred based on the requirement that the model response shall match the actual aircraft response.

Within this formulation, the problem can be solved by different methods, however, a variety of factors can make it difficult to apply these techniques in the real world. Among the difficulties, one can list the following [9]:

- there is no perfect measurement;
- system is also excited by state noise; and
- proposed model is not fully representative of the actual aircraft.

The aircraft dynamics can be described by the following general model [9]:

$$\begin{aligned} \dot{\mathbf{x}}(t) &= f(\mathbf{x}(t),\mathbf{u}(t),\theta) + \mathbf{w}(t) \\ \mathbf{x}(0) &= x_0 \\ \mathbf{y}(t) &= g(\mathbf{x}(t),\mathbf{u}(t),\theta) \\ \mathbf{z}(i) &= \mathbf{y}(i) + \mathbf{v}(i) \end{aligned} \tag{6}$$

The functions $\boldsymbol{f}$ and $\boldsymbol{g}$ are general real valued vector differentiable functions; $\boldsymbol{x}$(t) is the state vector; $\boldsymbol{y}$(t) is the proposed model; and $\boldsymbol{z}$(i) is the measurement vector.

In a discrete model, the state noise ***w***(i) vector is assumed to be zero-mean white Gaussian and stationary with variance ***Q***. The discrete measurement noise vector ***v***(i) is assumed to be zero mean white Gaussian and band limited, such that:

$$E\{\mathbf{v}(i)\} = 0 \qquad E\{\mathbf{w}(i)\} = 0$$
$$E\{\mathbf{v}(i)\mathbf{v}(i)^T\} = \mathbf{R}\delta_{ij} \quad E\{\mathbf{w}(i)\mathbf{w}(i)^T\} = \mathbf{Q}\delta_{ij} \tag{7}$$

There are various methods to estimate flight derivatives, considering the characteristics of both process and measurement noise associated with confidence on process model and output model as well. The Maximum Likelihood is a well-established method to do a parameter estimation based on the estimated output error, thus it is a strong candidate to be selected. It estimates the parameter vector that maximises the conditional probability density function:

$$\hat{\theta} = \arg\max_{\theta}[p(Z/\theta)] \tag{8}$$

where Z is the set of all measurement vector, for i=1,2,3,…,N. When R is known, maximising the conditional probability in the following equation is equivalent to minimising the cost function [10]:

$$J(\theta) = \frac{1}{2}\sum_{i=1}^{N}[\mathbf{z}(i) - \mathbf{y}(i)]^T \mathbf{R}^{-1}[\mathbf{z}(i) - \mathbf{y}(i)] \tag{9}$$

In addition, the following assumptions are made for this experiment:

- Flight Mach ≤ 2;
- A post flight data analysis is performed;
- Adequate vehicle conditions prior to excitation:
- Angular rates (stability);
- Distance from coast;
- Heading;
- Distance from telemetry station;
- Command surface position (below 75% range limit).
- Excitation characteristics:
- Multistep waveform scaled to achieve adequate vehicle response;
- Cycle: around 30 seconds each excitation cycle (ideal 3 cycles)
- Excitations inputs are added to control commands;
- Inputs design based on predicted vehicle dynamics; and
- Amplitude modulated to generate enough dynamics.

Multistep excitation (Fig. 5) has the characteristics of containing a high frequency spectrum. This manoeuvre should be designed to match the frequency bandwidth of vehicle dynamics, and to excite the vehicle in a proper level not to exceed response amplitudes, exciting nonlinearities, but, at the same time, providing adequate output signal to noise ratio. The excitation architecture should be additive to vehicle control, in a sense that flight controls are maintained fully operational during the PID manoeuvres, as shown in Fig. 4.

The flight test instrumentation should contain information from multiple sensors at a minimum sampling rate of 25Hz. Relevant information is: accelerations (a_x, a_y, a_z); angular rates (p, q, r); attitudes (Phi, Theta, Psi); position (X, Y, Z GPS); input deflections (δe, δa); estimated (M, V, α and β).

Aerodynamic derivatives candidates to be investigated are the parameters to be identified by the identification method. Modelling aircraft behaviour should consider longitudinal, lateral-directional dynamics and eventually both dynamics coupling. A linear aerodynamic model should be adequate to describe the measured data [11, 12]. Primary derivatives of interest are:

- Longitudinal:
  - Lift derivatives: CL_{α}, $CL_{\delta e}$;
  - Drag derivatives: CD_{α}, $CD_{\delta e}$;
  - Pitch moment derivatives: Cm_{α}, Cm_{q}, $Cm_{\delta e}$.
- Lateral-Directional:
  - Lateral force derivatives: CY_{β};
  - Rolling moment: Cl_{β}, $Cl_{\delta a}$, Cl_{p};
  - Yawing moment: Cn_{β}, $Cn_{\delta a}$, Cn_{r}.

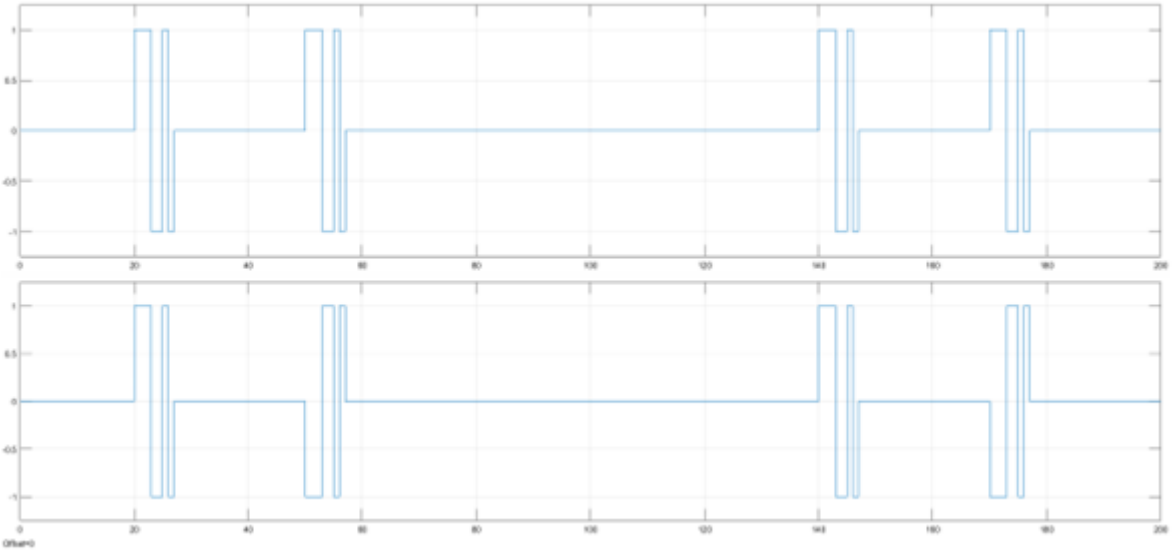

Fig 5 – Illustrative multistep excitation signal.

3. Results

3.1. Mesh convergence studies

In this section, aerodynamic coefficients of the EFTV flying at Mach number 2.0, determined using two mesh sizes, are shown: the regular mesh has 7.6 million elements, and the refined mesh has 22.7 million. In both cases, 2nd-order discretisation is used. The studies considered both the density and pressure-based solvers to evaluate the solution of each one at both meshes. Atmospheric conditions imposed were the pressure of 5,206.06 Pa and temperature of 216.97 K, which are related to 20,385 m of altitude. One example of the mesh generated for this convergence analysis is presented in Fig. 6.

The simulation results for drag and lift coefficients are presented in Table 1. Comparing results for 0 deg. of elevon deflection angle, one can verify that the difference in results obtained by the two solvers for the refined mesh (22.7 million elements) is negligible. Additionally, the relative difference between the results obtained with the regular mesh (about 7.6 million elements) compared to the refined one are less than 2%.

For a minus 5 deg deflection angle the difference between the two solvers is less than 0.5%. The relative difference between regular and refined meshes is less than 2.2 %.

For the regular meshes, the maximum difference found using the two solvers is 3.7% for 0 deg deflection angle and 3.9% for 5 deg. Both solvers give compatible results for Mach number less than 2, but the computational effort using the pressure-based solver is far smaller. The pressure-based solver and the regular meshes were adopted for all subsequent CFD simulations on Mach number 1.35.

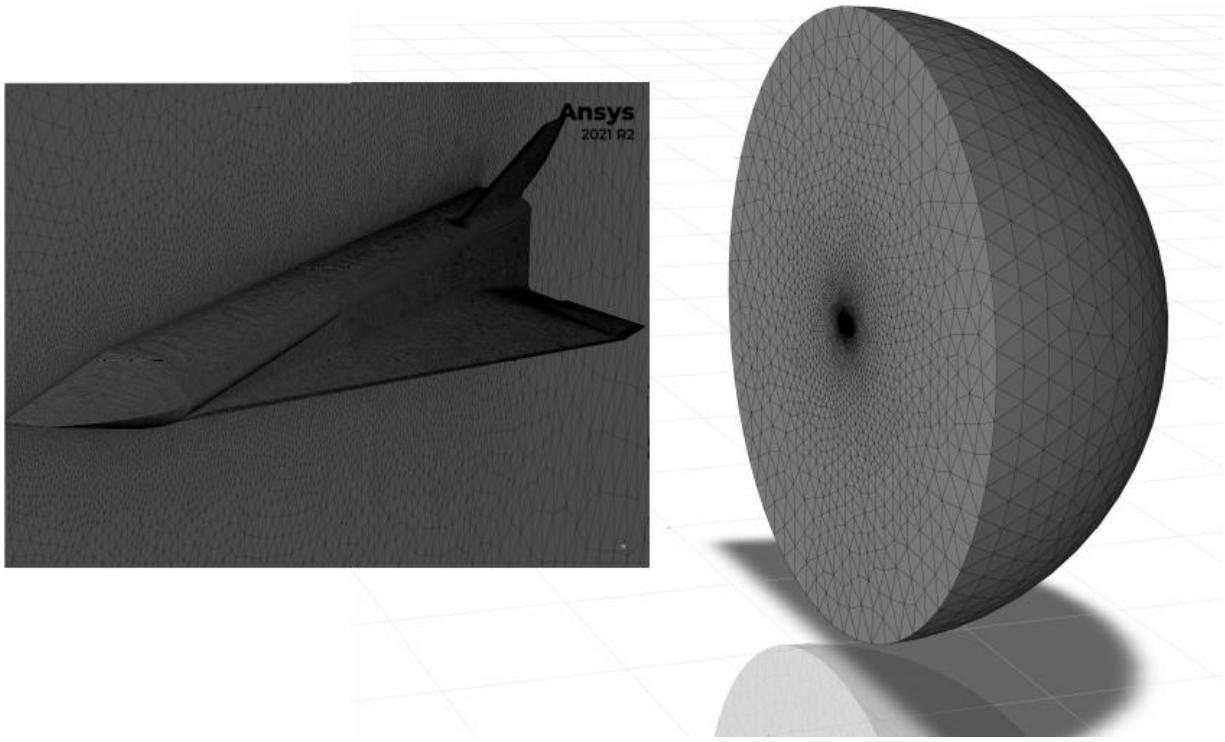

Fig 6 – Mesh and domain used in convergence analysis.

Table 1. Convergence results for Mach 2.0

Solver	Flight conditions		Aerodynamic Coeff.	Regular Mesh	Refined Mesh	Relative difference (%)
	α (deg)	δ (deg)				
Density-based	0.0	0.0	C_L	0.07115	0.07069	0.6
Density-based	0.0	0.0	C_D	0.03432	0.03377	1.6
Density-based	0.0	-5.0	C_L	0.05761	0.05752	0.2
Density-based	0.0	-5.0	C_D	0.03279	0.03233	1.4
Pressure-based	0.0	0.0	C_L	0.07077	0.07069	0.1
Pressure-based	0.0	0.0	C_D	0.03311	0.03377	-2.0
Pressure-based	0.0	-5.0	C_L	0.05747	0.05726	0.4
Pressure-based	0.0	-5.0	C_D	0.03156	0.03228	-2.2

3.2. CFD code-to-code comparison

This section compares some results for Mach number 2 and different flight conditions with previous results registered in the AEDB. Table 2 shows some of the aerodynamic coefficients computed using in-house second-order discretisation mesh compared with the original AEDB. In all cases, the difference is below 10%.

However, we must emphasise that the results obtained using the AEDB mesh, Density-based solver, and 1st-order discretisation agree perfectly with the original database. The maximum difference found

in cases analysed is less than 0.5%. Table 3 presents some of these results. There was no convergence using 2nd-order discretisation with the density-based solver.

Table 2. Aerodynamic coefficients computed using in-house 2nd-order discretisation meshes: Mach number = 2.0

Case	Solver	Flight conditions		Aerodynamic Coeff.	In-house mesh	AEDB	Relative difference (%)
		α (deg)	δ (deg)				
38	Density-based	0.0	0.0	C_L	0.07115	0.06759	5.3
38	Pressure-based	0.0	0.0	C_L	0.07077	0.06759	4.7
39	Density-based	0.0	-5.0	C_L	0.05761	0.05359	7.5
39	Pressure-based	0.0	-5.0	C_L	0.05747	0.05359	7.2
44	Pressure-based	5.0	0.0	C_L	0.19438	0.18526	4.9
45	Pressure-based	5.0	-5.0	C_L	0.18167	0.17213	5.5
38	Density-based	0.0	0.0	C_D	0.03432	0.03654	-6.1
38	Pressure-based	0.0	0.0	C_D	0.03311	0.03654	-9.4
39	Density-based	0.0	-5.0	C_D	0.03279	0.03497	-6.2
39	Pressure-based	0.0	-5.0	C_D	0.03156	0.03497	-9.8
44	Pressure-based	5.0	0.0	C_D	0.05969	0.06125	-2.5
45	Pressure-based	5.0	-5.0	C_D	0.05614	0.05746	-2.3

However, we must emphasise that the results obtained using the AEDB mesh, Density-based solver, and 1st-order discretisation agree perfectly with the original database. The maximum difference found in cases analysed is less than 0.5%. Table 3 presents some of these results. There was no convergence using 2nd-order discretisation with the density-based solver.

Table 3. Aerodynamic coefficients computed using in-house 1st-order discretisation meshes: Mach number = 2.0

Case	Solver	Flight conditions		Aerodynamic Coeff.	In-house mesh	AEDB	Relative difference (%)
		α (deg)	δ (deg)				
37	Density-based	0.0	5.0	C_L	0.08263	0.08262	0.014
38	Density-based	0.0	0.0	C_L	0.06760	0.06759	0.016
39	Density-based	0.0	-5.0	C_L	0.05357	0.05359	-0.03
37	Density-based	0.0	5.0	C_D	0.04064	0.04063	0.028
38	Density-based	0.0	0.0	C_D	0.03655	0.03654	0.024
39	Density-based	0.0	-5.0	C_D	0.03496	0.03497	-0.011

3.3. Aerodynamic coefficients for Mach number 1.35

A large range of simulations was made comprising positive and negative angles of attack at the same flight conditions considered as the end of the original flight phase. The side-slip angle was considered zero and non-zero. For these conditions, the elevon was positioned at -10, -5, 0 and 5 degrees. Only a few results are presented in the following.

Simulation cases were developed aiming for the flight test to be performed at Mach number 1.35 and 15,884m of altitude. The pressure-based solver with 2nd-order spatial discretisation and Spalart-Allmaras turbulence method is used for all simulations. Two mesh schemes are used, one hemispherical for symmetrical deflection of elevons and a second scheme with full spherical mesh for asymmetrical deflection of elevons. The spherical mesh type was also used to simulate non-zero side-slip angles.

Fig. 7 shows the effect of changing the angle of attack (α) on aerodynamics coefficients for cases with symmetric elevon deflections (δ) and β= 0.

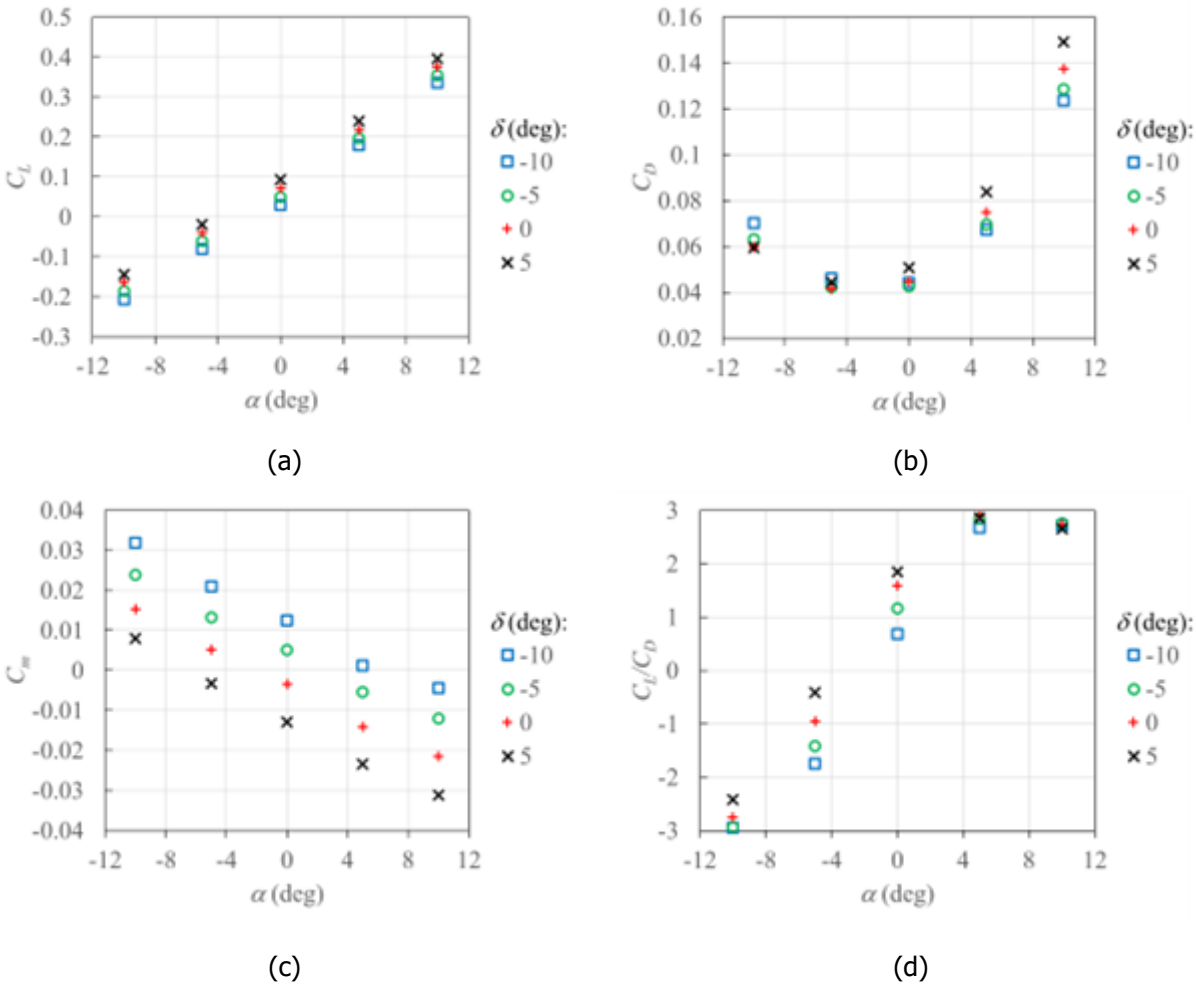

Fig 7 – Aerodynamic parameters as a function of angle of attack for several values of elevon deflection: (a) lift coefficient; (b) drag coefficient; (c) pitching moment coefficient; (d) aerodynamic efficiency.

Although references [4] and [5] show that the EFTV aerodynamic efficiency can reach values greater than 5 for Mach number 8, its maximum value for Mach number 1.35 drops to approximately 2.9, which is associated with α = 5 deg, as indicated in Fig. 7.

In Fig. 8, the effect of changing the left elevon deflection (δ), while the right elevon is kept deflected at 5 deg, is shown on aerodynamic coefficients and efficiency.

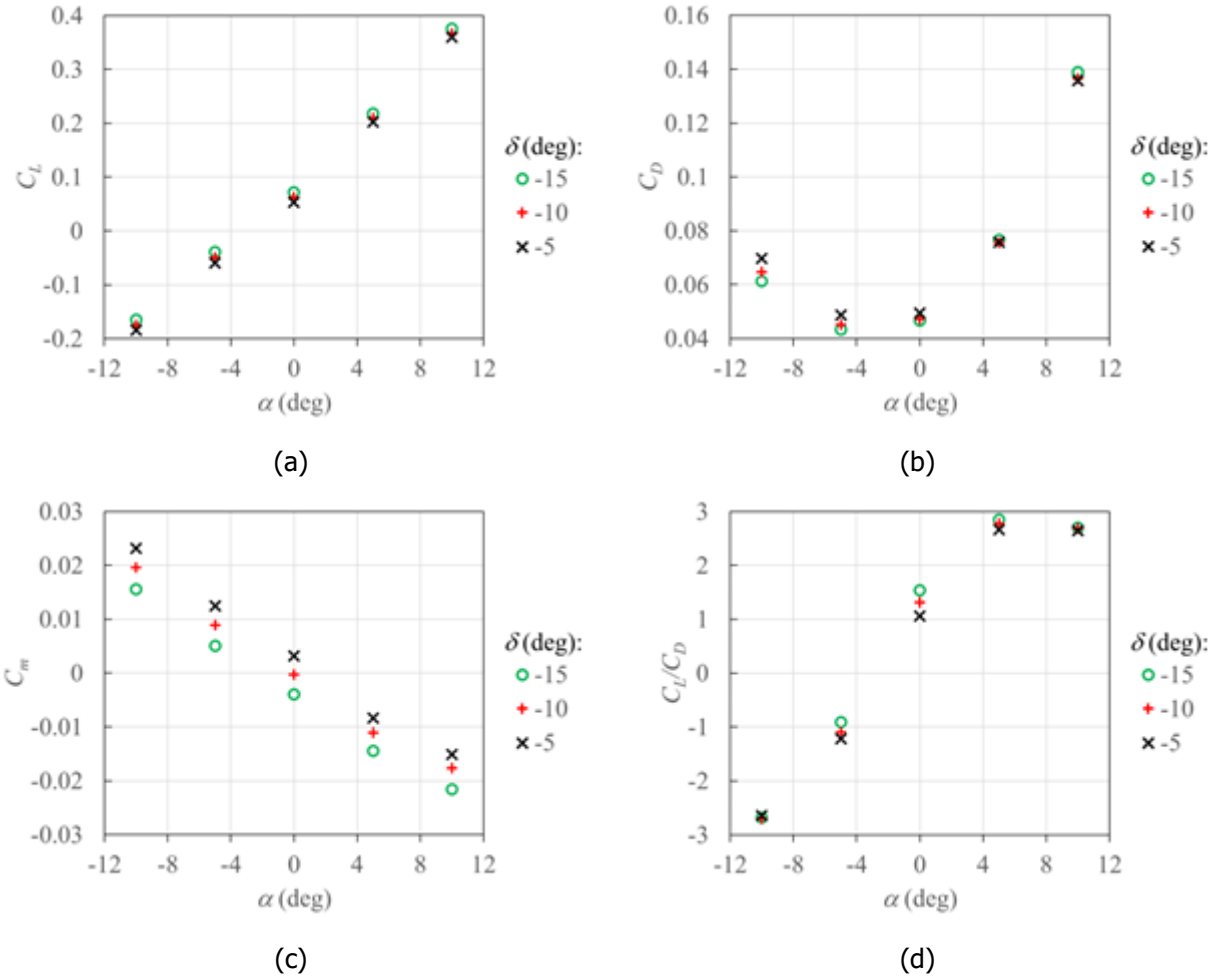

Fig 8 – Aerodynamic parameters as a function of angle of attack for several values of left elevon deflection (right elevon deflection = 5 deg): (a) lift coefficient; (b) drag coefficient; (c) pitching moment coefficient; (d) aerodynamic efficiency.

The results presented in Fig. 8 show that the effect of changing the left elevon deflection while the right one is kept at 5 deg has no relevant impact on force coefficients. Although the maximum aerodynamic efficiency (2.85) was obtained for left elevon deflection of -15 deg, it is still 2% lower than the maximum value shown in Fig. 7(d).

Fig. 9 shows the effect of changing both α and β on aerodynamic coefficients and efficiency for the configuration in which both elevons are not deflected. When β is increased from zero to 4 deg, the most significant effect is observed on coefficients C_L and C_n. On the other hand, the impact of β on drag and lift coefficients is not significant.

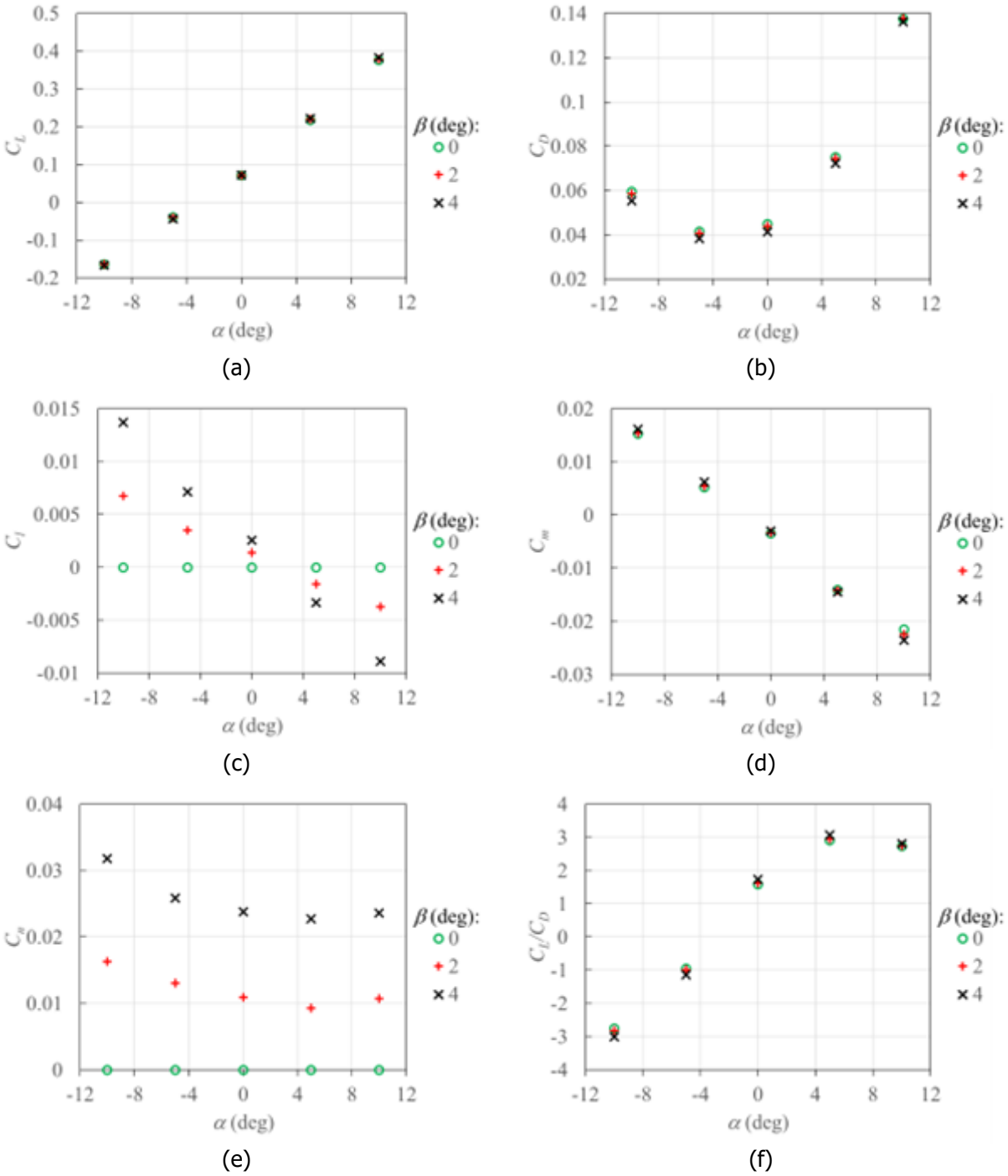

Fig 9 – Aerodynamic parameters as a function of angle of attack and angle of sideslip: (a) lift coefficient; (b) drag coefficient; (c) rolling moment coefficient; (d) pitching moment coefficient; (e) yawing moment coefficient; (f) aerodynamic efficiency.

4. Future Work

The next steps of this experiment are still an on-going activity and include the computation of more aerodynamic coefficients, the numerical stability derivatives using the VLM, followed by the development of the glider flight controller for Mach below 2 and the planning of the multistep input signal for the parameter identification manoeuvre. A robust linear controller and the ideal amplitudes for each PID signal will be developed and tested using the flight simulation environment created in Matlab Simulink.

References

[1] Steelant J., Villace V., Kallenbach A., Wagner A., Andro J.-Y., di Benedetto S., Saracoglu B. Chernyshev S.L., Gubanov A. A., Talyzin V. A., Voevodenko N. V., Kukshinov N.V., Prokhorov A. N., Grigoriev N. V., Neely A. J., Verstraete D. and Buttwsorth D., 'Flight Testing Designs in HEXAFLY-INT for High-Speed Transportation', 1st International Conference on High-Speed Vehicle Science and Technology (HiSST), HiSST-2018-3101064, 26-29/11/2018, Moscow, Russia.

[2] Di Benedetto, S., Di Donato, M. P. D., Rispoli, A., Pezzella, G., Scigliano, R., Nebula, F., Cristillo, D., Marini, M., Cardone, S., Steelant, J., Villace, V. Vecchione, L.: Multidisciplinary Design and Flight Test of the HEXAFLY-INT Experimental Flight Vehicle," *HiSST: International Conference on High-Speed Vehicle Science Technology,* 26-29 November 2018.

[3] Di Benedetto S., Di Donato, M.-P., Schettino A., Scigliano R., Nebula F., Morani G., Cristillo D., Marini M., Cardone S., Steelant J., Villace V.F., 'The High-Speed Experimental Flight Test Vehicle of HEXAFLY-INT: a Multidisciplinary Design', CEAS Space Journal, Feb 2020.

[4] Pezzella, G., Marini, M., Reimann, B., Steelant, J. , Aerodynamic Design Analysis of the HEXAFLY-INT Hypersonic Glider, *20th AIAA International Space Planes and Hypersonic Systems and Technologies Conference,* 2015. https://doi.org/10.2514/6.2015-3644

[4] Schettino A., Pezzella G., Marini M., Di Benedetto S., Fernandez-Villace V., Steelant J., Choudhury, R., Gubanov A. and Voevodenko N., Aerodynamic Database of the HEXAFLY-INT Hypersonic Glider, CEAS Space Journal, Feb. 2020, doi.org/10.1007/s12567-020-00299-4.

[5] Steelant J., Passaro A., Fernandez-Villace V., Gubanov A.A., Shvalyov Y.G., Ivanyuskhin D.S., Voevodenko N.V., Marini M. and di Benedetto S., 'Boundary Layer Transition Assessment on a Slender High-Speed Vehicle', 21st Int. Space Planes and Hypersonic Systems and Technology Conference, AIAA-2017-2133, 6-9 March 2017, Xiamen, China.

[6] Center, N.G.D., "US Standard Atmosphere (1976)," *Planetary and Science, Vol. 40, No. 4,* pp. 553-554, 1992.

[7] Spalart, P., Allmaras, S.: A one-equation turbulence model for aerodynamic flows, *30th Aerospace Sciences Meeting and Exhibit,* 1992. https://doi.org/10.2514/6.1992-439

[8] Stevens, B.L., Lewis, F.L.: Aircraft Control and Simulation. John Wiley& Sons (1992)

[9] Mendonça, C. B., Hemerly, E. M., and Goes, L. C. S.: Adaptive Stochastic Filtering for On-Line Aircraft Flight Path Reconstruction, AIAA Journal of Aircraft, Vol. 44, No. 5, 2007, pp. 1546–1558. doi:10.2514/1.27625

[10] Jategaonkar, R. V.: Flight Vehicle System Identification: A Time Domain Methodology, Vol. 216, AIAA Progress in Astronautics and Aeronautics Series, AIAA, Reston, VA (2006).

[11] Klein, V., Morelli, E.A.: Aircraft System Identification – Theory and Practice, AIAA Education Series, AIAA, Reston, VA (2016).

[12] Morelli, E.A., Derry, S.D.: Aerodynamic Parameter Estimation for the X-43A (Hyper-X) from Flight Data. AIAA Atmospheric Flight Mechanics Conference and Exhibit August 15-18, 2005 / San Francisco, CA.